Supporting Information

for

Aggregation-induced emission of boryl substituted phenothiazine: synthesis and applications in fluoride ions sensing

Yan Wang,[‡, a] *Guoqiang Li,*[‡, a] *Zengheng Wen,*[a] *Zhuang Luo,*[a] *Qiangqiang Jia*[*b] *and Weidong Zhang*[*a]

[a] School of Chemical Engineering, Qinghai University, Xining, 810016, China
E-mail: zhangwd@qhu.edu.cn

[b] *State Key Laboratory of Plateau Ecology and Agriculture, Qinghai University, Xining, 810016, China*
E-mail: jia1108029@163.com

Contents

1. The excitation and emission spectra

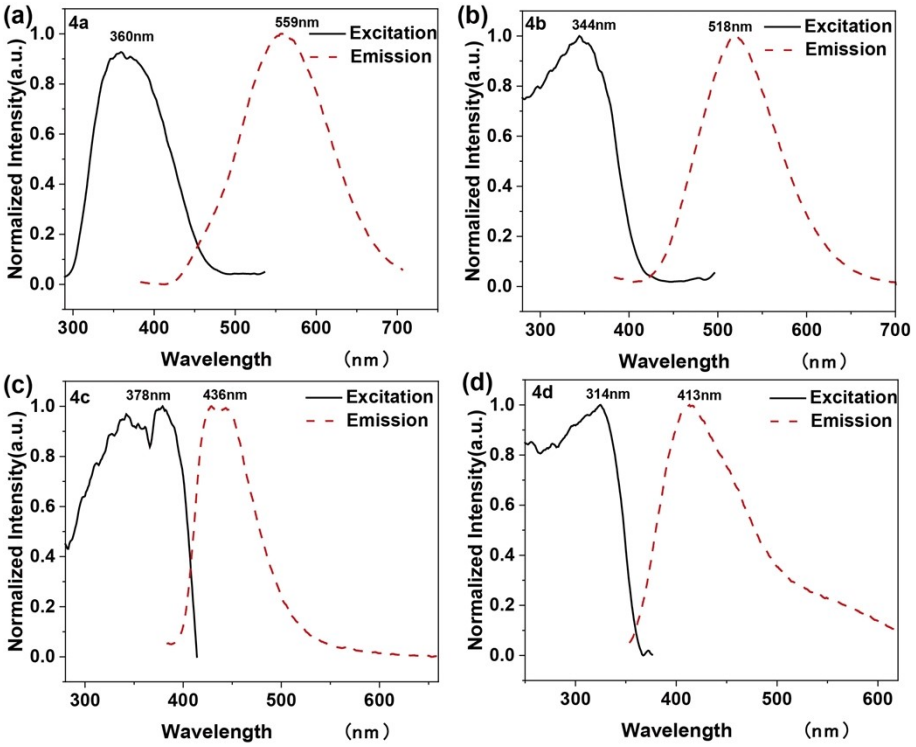

Figure S1. Fluorescence excitation (solid line) and emission spectra (dashed line).

2. The **fluorescence lifetime decay spectra**

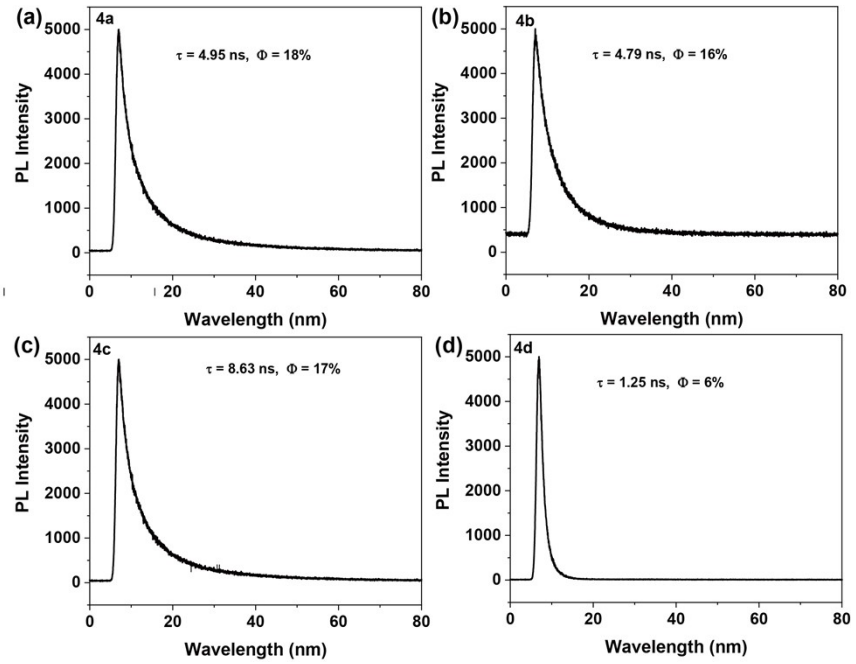

Figure S2. Fluorescence lifetime decay spectra of **4a-4d**.

3. The Experimental and the Calculated UV-Vis spectra

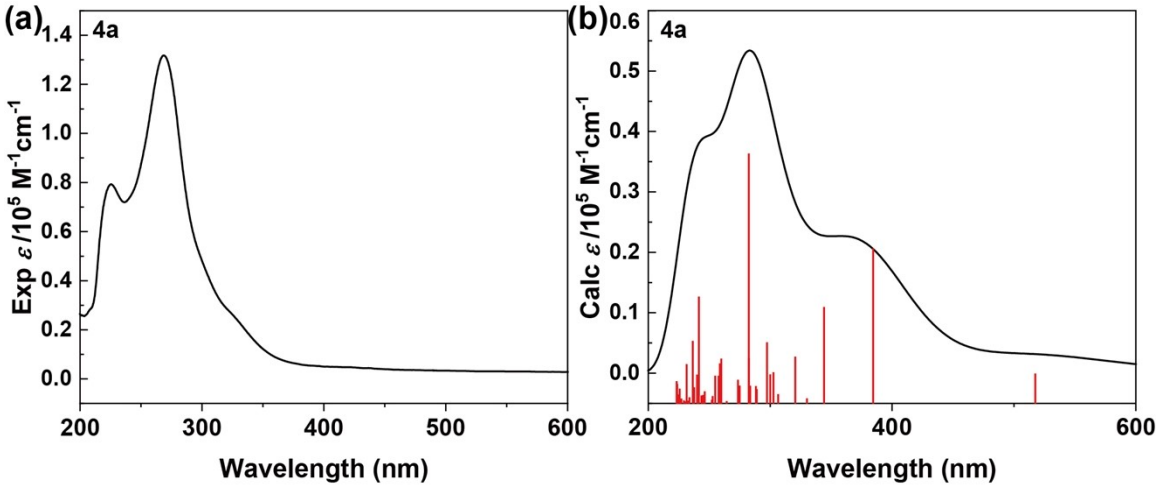

Figure S3. Computed, at the TD-DFT, B3LYP-D3/6-31g(d),[1-4] level of theory and experimental UV-vis spectra of **4a**.

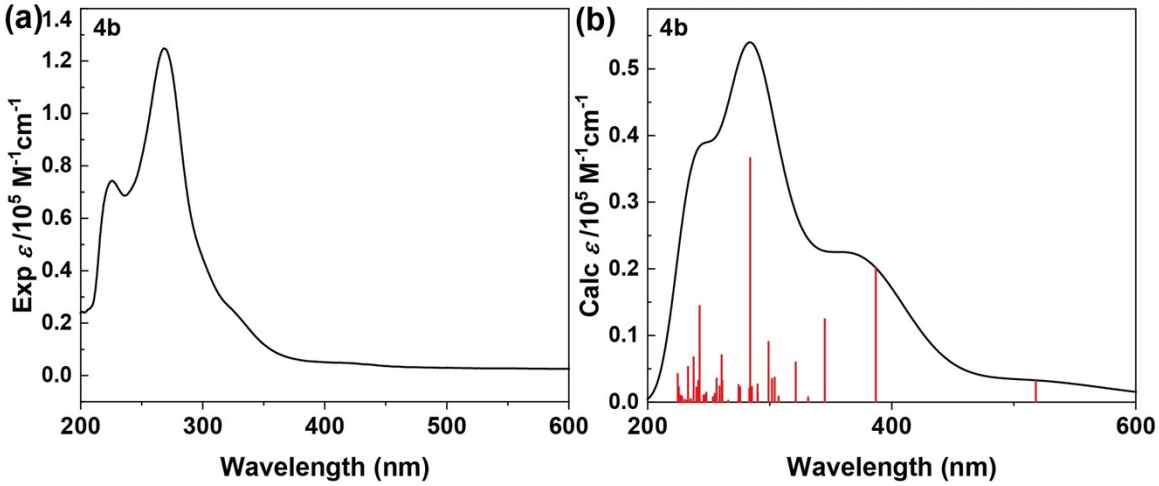

Figure S4. Computed, at the TD-DFT, B3LYP-D3/6-31g(d), level of theory and experimental UV-vis spectra of **4b**.

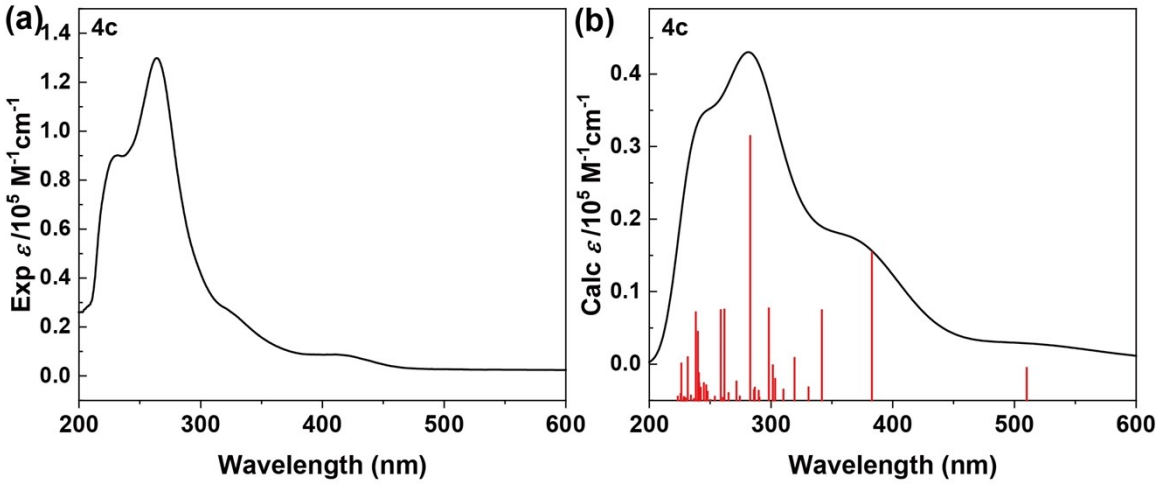

Figure S5. Computed, at the TD-DFT, B3LYP-D3/6-31g(d), level of theory and experimental UV-vis spectra of **4c**.

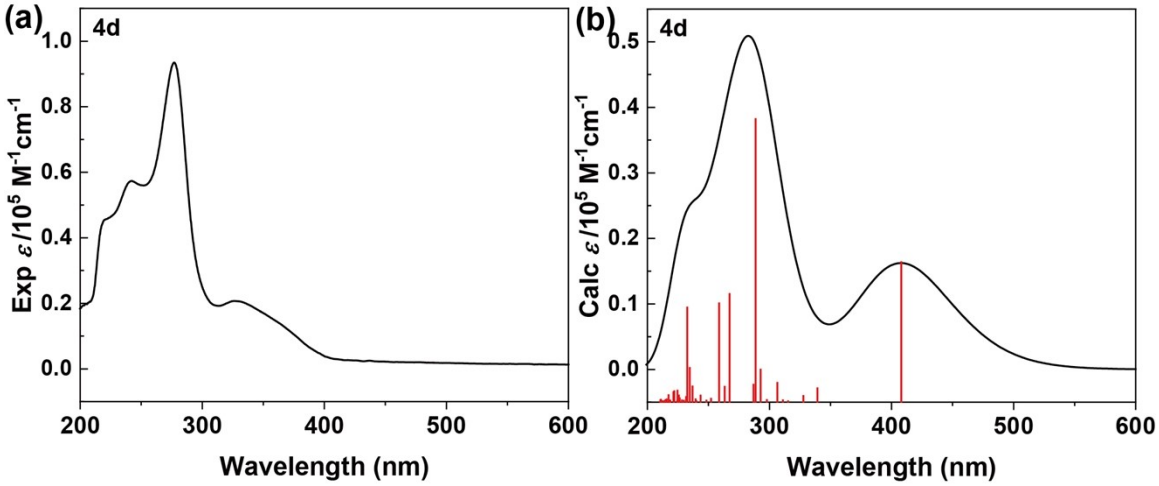

Figure S6. Computed, at the TD-DFT, B3LYP-D3/6-31g(d), level of theory and experimental UV-vis spectra of **4d**.

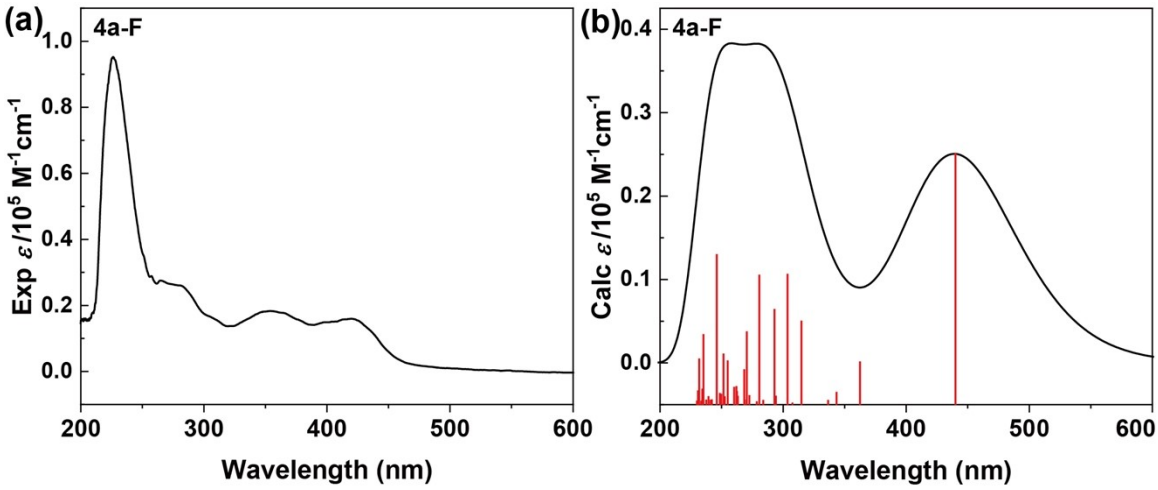

Figure S7. Computed, at the TD-DFT, B3LYP-D3/6-31g(d), level of theory and experimental UV-vis spectra of **4a-F**.

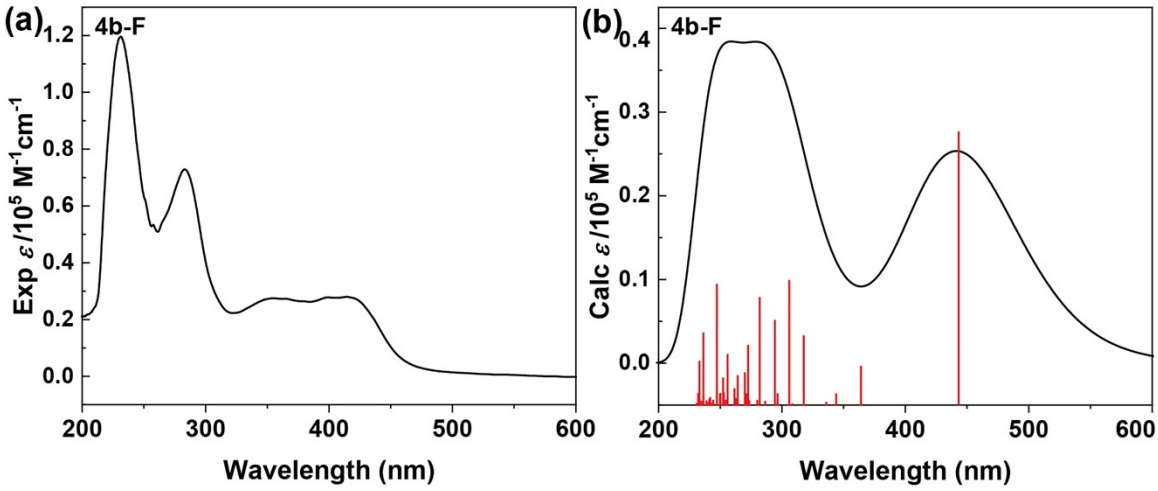

Figure S8 Computed, at the TD-DFT, B3LYP-D3/6-31g(d), level of theory and experimental UV-vis spectra of **4b-F**.

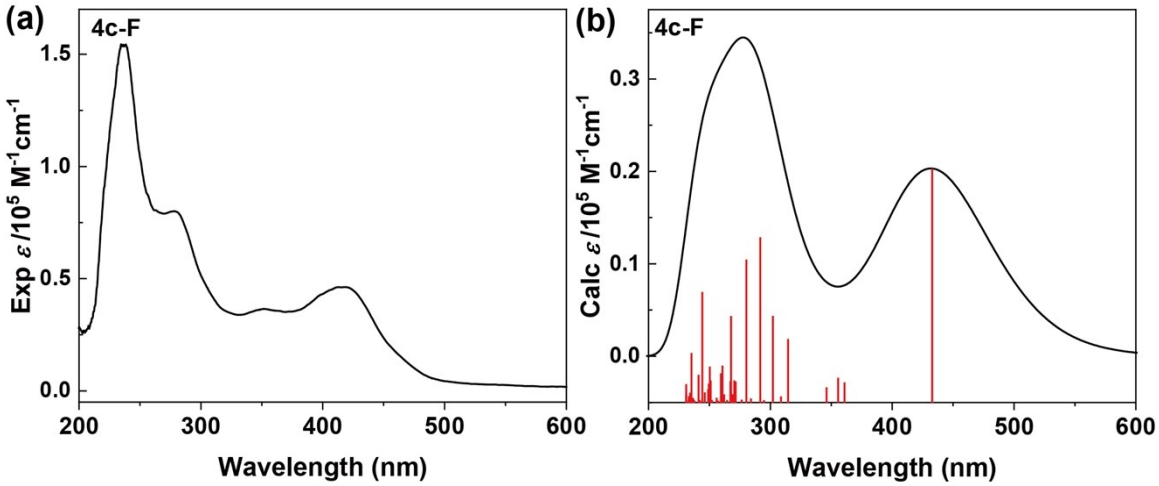

Figure S9 Computed, at the TD-DFT, B3LYP-D3/6-31g(d), level of theory and experimental UV-vis spectra of **4c-F**.

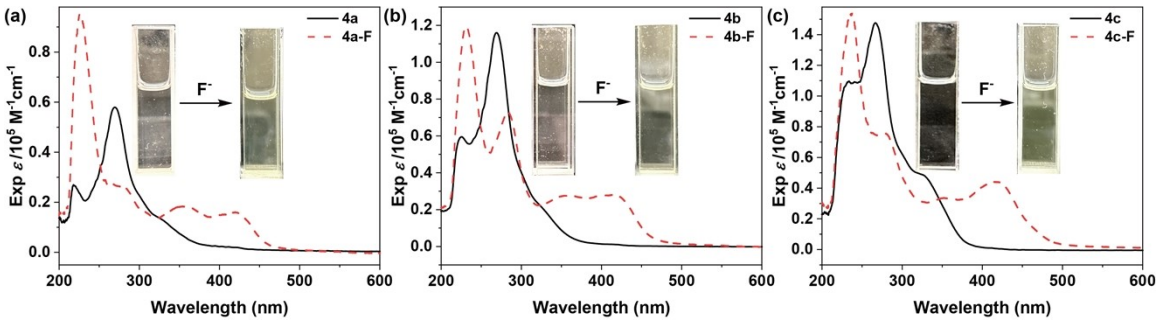

Figure S10. UV-Vis absorption spectral and solution colors of **4a-4c** changes after the addition of TBAF.

Table S1. Calculated ($\lambda_{TD\text{-}DFT}$) wavelengths of **4a**. Molecular orbitals (MOs) involved in the main electronic transition，f corresponds to the oscillator strength. (TD-DFT, B3LYP-D3/6-31g(d))

$\lambda_{TD\text{-}DFT}$	Oscillator Strength, f	MOs	
385.17	0.3909	HOMO-1 ->LOMO	16.01%
		HOMO ->LOMO+1	68.02%
344.84	0.2411	HOMO-1 ->LOMO	66.14%
		HOMO ->LOMO+1	15.69%
		HOMO ->LOMO+2	12.26%
321.23	0.1147	HOMO-3 ->LOMO	18.10%
		HOMO-2 ->LOMO	58.86%
		HOMO ->LOMO+2	29.39%
		HOMO ->LOMO+3	12.45%
298.15	0.1512	HOMO-5 ->LOMO	28.20%
		HOMO-4 ->LOMO	49.77%
		HOMO-3 ->LOMO	24.74%
		HOMO-2 ->LOMO	11.54%
		HOMO ->LOMO+3	20.36%
		HOMO ->LOMO+4	12.82%
283.25	0.1110	HOMO-6 ->LOMO	24.28%
		HOMO-1 ->LOMO+1	22.78%
		HOMO ->LOMO+5	57.60%
283.11	0.6319	HOMO-1 ->LOMO+1	54.17%
		HOMO ->LOMO+4	27.26%
		HOMO ->LOMO+5	21.24%
		HOMO ->LOMO+6	11.33%
		HOMO ->LOMO+8	19.26%
260.53	0.1099	HOMO-9 ->LOMO	16.95%
		HOMO-8 ->LOMO	14.27%
		HOMO-7 ->LOMO	13.71%
		HOMO-2 ->LOMO+1	57.35%
		HOMO-1 ->LOMO+2	14.04%
		HOMO ->LOMO+9	14.03%
		HOMO ->LOMO+10	14.89%
242.26	0.2677	HOMO-2 ->LOMO+2	62.15%
		HOMO-2 ->LOMO+3	15.10%
		HOMO-1 ->LOMO+3	14.80%

Table S2. Calculated ($\lambda_{TD\text{-}DFT}$) wavelengths of **4b**. Molecular orbitals (MOs) involved in the main electronic transition，f corresponds to the oscillator strength. (TD-DFT, B3LYP-D3/6-31g(d))

$\lambda_{TD\text{-}DFT}$	Oscillator Strength, f	MOs	
386.03	0.3942	HOMO-1 ->LOMO	15.57%
		HOMO ->LOMO+1	68.15%
344.38	0.2416	HOMO-1 ->LOMO	66.19%
		HOMO ->LOMO+1	15.24%
		HOMO ->LOMO+2	12.51%
320.41	0.1151	HOMO-3 ->LOMO	18.87%
		HOMO-2 ->LOMO	60.33%
		HOMO ->LOMO+2	25.92%
		HOMO ->LOMO+3	11.24%
		HOMO-3 ->LOMO	44.56%
		HOMO ->LOMO+3	25.59%
298.17	0.1754	HOMO-5 ->LOMO	30.63%
		HOMO-4 ->LOMO	48.57%
		HOMO-3 ->LOMO	23.83%
		HOMO-2 ->LOMO	12.80%
		HOMO ->LOMO+3	20.73%
		HOMO ->LOMO+4	11.79%
		HOMO-5 ->LOMO	10.31%
283.17	0.7125	HOMO-1 ->LOMO+1	57.57%
		HOMO ->LOMO+4	28.11%
		HOMO ->LOMO+5	13.37%
		HOMO ->LOMO+8	14.39%
259.81	0.1359	HOMO-9 ->LOMO	12.04%
		HOMO-8 ->LOMO	44.67%
		HOMO-2 ->LOMO+1	39.74%
		HOMO ->LOMO+10	25.44%
241.78	0.2799	HOMO-2 ->LOMO+2	62.52%
		HOMO-2 ->LOMO+3	14.88%
		HOMO-1 ->LOMO+3	13.67%
236.84	0.1303	HOMO-7 ->LOMO+1	25.26%
		HOMO-2 ->LOMO+2	22.75%
		HOMO-2 ->LOMO+3	10.38%
		HOMO-1 ->LOMO+3	29.21%
		HOMO-1 ->LOMO+4	42.68%

Table S3. Calculated ($\lambda_{TD\text{-}DFT}$) wavelengths of **4c**. Molecular orbitals (MOs) involved in the main electronic transition，f corresponds to the oscillator strength. (TD-DFT, B3LYP-D3/6-31g(d))

$\lambda_{TD\text{-}DFT}$	Oscillator Strength, f	MOs	
382.20	0.3024	HOMO-1 ->LOMO	16.84%
		HOMO ->LOMO+1	67.74%
341.09	0.1839	HOMO-1 ->LOMO	63.96%
		HOMO ->LOMO+1	15.98%
		HOMO ->LOMO+2	19.00%
297.44	0.1875	HOMO-5 ->LOMO	37.59%
		HOMO-4 ->LOMO	39.35%
		HOMO-3 ->LOMO	21.79%
		HOMO-2 ->LOMO	15.64%
		HOMO ->LOMO+2	11.13%
		HOMO ->LOMO+3	25.75%
		HOMO ->LOMO+4	15.05%
282.19	0.5398	HOMO-1 ->LOMO+1	61.72%
		HOMO ->LOMO+4	22.59%
		HOMO ->LOMO+5	10.40%
		HOMO ->LOMO+8	12.57%
261.00	0.1854	HOMO-10 ->LOMO	13.60%
		HOMO-7 ->LOMO	14.80%
		HOMO-1 ->LOMO+1	14.03%
		HOMO ->LOMO+8	30.88%
		HOMO ->LOMO+10	54.28%
257.97	0.1841	HOMO-3 ->LOMO+1	18.90%
		HOMO-2 ->LOMO+1	59.85%
		HOMO ->LOMO+9	17.74%
		HOMO ->LOMO+10	10.14%
237.50	0.1800	HOMO-10 ->LOMO	16.90%
		HOMO-9 ->LOMO	15.24%
		HOMO-8 ->LOMO	12.56%
		HOMO-2 ->LOMO+2	21.75%
		HOMO-1 ->LOMO+3	47.99%
		HOMO-1 ->LOMO+4	31.56%

Table S4. Calculated ($\lambda_{TD\text{-}DFT}$) wavelengths of **4d**. Molecular orbitals (MOs) involved in the main electronic transition，f corresponds to the oscillator strength. (TD-DFT, B3LYP-D3/6-31g(d))

$\lambda_{TD\text{-}DFT}$	Oscillator Strength, f	MOs	
408.71	0.3965	HOMO ->LUMO	69.60%
289.37	0.8039	HOMO-1 ->LOMO	54.85%
		HOMO ->LOMO+5	26.61%
		HOMO ->LOMO+6	13.63%
		HOMO ->LOMO+7	27.15%
267.99	0.3061	HOMO-1 ->LOMO	14.79%
		HOMO ->LOMO+8	56.44%
		HOMO ->LOMO+9	28.35%
		HOMO ->LOMO+10	20.46%
259.43	0.2795	HOMO-2 ->LOMO	59.92%
		HOMO ->LOMO+2	11.34%
		HOMO ->LOMO+9	17.51%
		HOMO ->LOMO+10	23.84%
233.35	0.2677	HOMO-4 ->LOMO	10.80%
		HOMO-2 ->LOMO+2	52.20%
		HOMO-1 ->LOMO+4	11.62%
		HOMO-1 ->LOMO+5	34.31%
		HOMO-1 ->LOMO+7	12.55%

Table S5. Calculated ($\lambda_{TD\text{-}DFT}$) wavelengths of **4a-F**. Molecular orbitals (MOs) involved in the main electronic transition，f corresponds to the oscillator strength. (TD-DFT, B3LYP-D3/6-31g(d))

$\lambda_{TD\text{-}DFT}$	Oscillator Strength, f	MOs	
440.79	0.6091	HOMO ->LUMO	70.02%
315.66	0.1664	HOMO-2 ->LOMO	10.39%
		HOMO-1 ->LOMO	65.44%
		HOMO ->LOMO+2	14.87%
		HOMO ->LOMO+4	11.13%
304.38	0.2606	HOMO-2 ->LOMO	64.08%
		HOMO-1 ->LOMO	14.13%
		HOMO ->LOMO+6	15.59%
293.79	0.1899	HOMO-3 ->LOMO	52.12%
		HOMO ->LOMO+4	42.44%
		HOMO ->LOMO+5	12.16%
281.50	0.2590	HOMO-4 ->LOMO	37.53%
		HOMO-1 ->LOMO+1	17.685
		HOMO ->LOMO+5	37.70%
		HOMO ->LOMO+6	35.15%
		HOMO ->LOMO+7	14.73%
271.30	0.1448	HOMO-7 ->LOMO	22.19%
		HOMO-6 ->LOMO	10.31%
		HOMO-5 ->LOMO	63.29%
		HOMO-2 ->LOMO+1	10.16%
246.88	0.3004	HOMO-5 ->LOMO+1	65.825
		HOMO-2 ->LOMO+3	11.08%
		HOMO ->LOMO+13	10.71%
235.97	0.1392	HOMO-8 ->LOMO	25.76%
		HOMO-7 ->LOMO+1	29.13%
		HOMO-5 ->LOMO+2	25.51%
		HOMO-4 ->LOMO+2	14.88%
		HOMO-2 ->LOMO+5	13.38%
		HOMO-2 ->LOMO+6	16.82%
		HOMO-1 ->LOMO+4	18.45%
		HOMO-1 ->LOMO+5	20.11%
		HOMO-1 ->LOMO+6	17.34%

Table S6 Calculated ($\lambda_{TD\text{-}DFT}$) wavelengths of **4b-F**. Molecular orbitals (MOs) involved in the main electronic transition，f corresponds to the oscillator strength. (TD-DFT, B3LYP-D3/6-31g(d))

$\lambda_{TD\text{-}DFT}$	Oscillator Strength, f	MOs	
442.87	0.6167	HOMO ->LUMO	70.04%
317.36	0.1554	HOMO-1 ->LOMO	65.97%
		HOMO ->LOMO+2	14.45%
		HOMO ->LOMO+4	10.26%
305.59	0.2805	HOMO-2 ->LOMO	63.28%
		HOMO-1 ->LOMO	12.20%
		HOMO ->LOMO+6	19.07%
293.98	0.1902	HOMO-3 ->LOMO	22.89%
		HOMO ->LOMO+4	60.14%
		HOMO ->LOMO+5	14.95%
		HOMO ->LOMO+6	15.83%
281.68	0.2419	HOMO-4 ->LOMO	24.61%
		HOMO-3 ->LOMO	10.81%
		HOMO-2 ->LOMO+1	11.26%
		HOMO-1 ->LOMO+1	34.49%
		HOMO ->LOMO+5	33.56%
		HOMO ->LOMO+6	34.39%
		HOMO ->LOMO+7	33.56%
272.31	0.1335	HOMO-7 ->LOMO	19.84%
		HOMO-5 ->LOMO	64.98%
		HOMO ->LOMO+7	10.15%
255.67	0.1129	HOMO-7 ->LOMO	51.40%
		HOMO-5 ->LOMO	14.82%
		HOMO-3 ->LOMO+3	13.98%
		HOMO-2 ->LOMO+3	26.92%
		HOMO-1 ->LOMO+2	15.42%
		HOMO-1 ->LOMO+3	17.42%
		HOMO ->LOMO+12	10.82%
247.09	0.2718	HOMO-6 ->LOMO+1	24.31%
		HOMO-5 ->LOMO+1	61.56%
		HOMO-2 ->LOMO+2	12.45%

Table S7 Calculated ($\lambda_{TD\text{-}DFT}$) wavelengths of **4c-F**. Molecular orbitals (MOs) involved in the main electronic transition，f corresponds to the oscillator strength. (TD-DFT, B3LYP-D3/6-31g(d))

$\lambda_{TD\text{-}DFT}$	Oscillator Strength, f	MOs	
433.61	0.4922	HOMO ->LUMO	69.87%
302.73	0.1267	HOMO-3 ->LOMO	16.98%
		HOMO-2 ->LOMO	60.18%
		HOMO-1 ->LOMO	16.36%
		HOMO ->LOMO+4	12.20%
		HOMO ->LOMO+6	18.04%
		HOMO ->LOMO+7	12.02%
292.50	0.2664	HOMO-3 ->LOMO	41.50%
		HOMO ->LOMO+4	48.10%
		HOMO ->LOMO+5	23.29%
281.03	0.2269	HOMO-4 ->LOMO	33.37%
		HOMO-3 ->LOMO	16.40%
		HOMO-1 ->LOMO+1	14.82%
		HOMO ->LOMO+5	33.01%
		HOMO ->LOMO+6	42.65%
		HOMO ->LOMO+7	12.06%
244.90	0.1693	HOMO-6 ->LOMO+1	48.34%
		HOMO-5 ->LOMO+1	33.21%
		HOMO-4 ->LOMO+2	32.50%
236.04	0.0853	HOMO-8 ->LOMO	47.62%
		HOMO-7 ->LOMO+1	24.91%
		HOMO-6 ->LOMO+3	22.33%
		HOMO-5 ->LOMO+2	10.45%
		HOMO-5 ->LOMO+3	10.94%
		HOMO-1 ->LOMO+4	12.55%
		HOMO ->LOMO+11	17.08%

4. Electrochemical properties

Cyclic voltammograms were recorded with a Metrohm PGSTAT204 electrochemical analyzer using DCM. The CV cell consisted of a gold electrode, a Pt wire counter electrode, and an Ag/AgCl reference electrode. All measurements were performed using DCM solutions of samples with a concentration of 1 mM and 0.1 M $Bu_4N^+BF_6^-$ as a supporting electrolyte with a scan rate of 100 mVs^{-1}. Potentials are determined against a ferrocene/ferrocenyl ion couple (Fc/Fc^+).

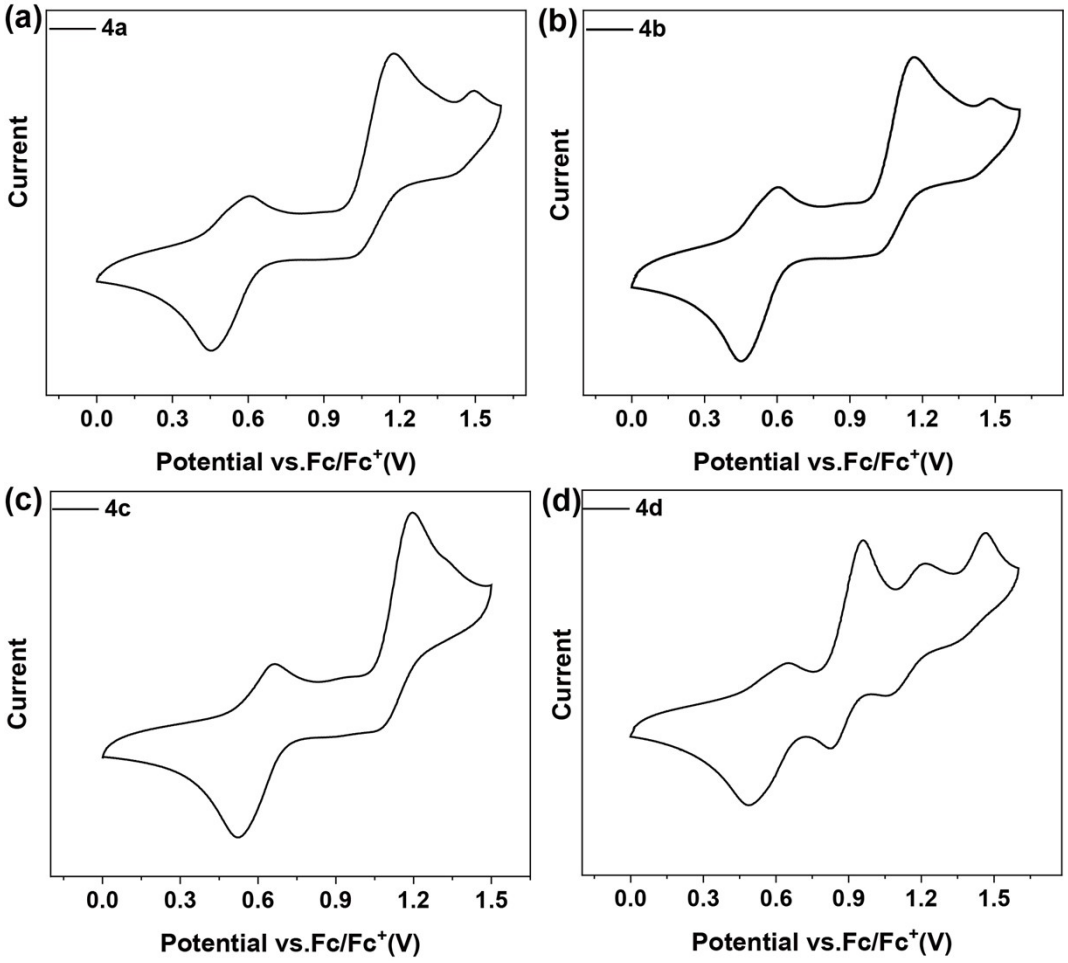

Figure S11. Cyclic voltammograms of **4a**, **4b**,**4c** and **4d** in DCM with $Bu_4N^+BF_6^-$ (0.1 M) as a supporting electrolyte, Fc = ferrocene.

5. Comparison of HOMO/LUMO plots

Table S8. ectronic properties of **4a**, **4b**, **4c** and **4d**

Entry	E_g[a](eV)	E_{OX}[b](V)	HOMO(eV) (Exp)[c]	LUMO(eV) (Exp)[d]	HOMO(eV) (Cal)[e]	LUMO(eV) (Cal)[e]	E_g (eV) (Cal)[e]
4a	4.24	1.00	-5.80	-1.56	-5.39	-0.93	4.46
4b	4.25	1.01	-5.81	-1.56	-5.40	-0.95	4.45
4c	4.28	1.05	-5.85	-1.57	-5.56	-1.08	4.48
4d	4.22	0.79	-5.59	-1.37	-5.04	-0.92	4.11

[a] E_g estimated from the UV-Vis absorption spectra.

[b] Oxidation onset potentials measured by cyclic voltammetry.

[c c] HOMO = -$(E_{OX} + 4.8)$ eV.

[d] LUMO = HOMO + E_g.

[e]Theoretical calculations have been carried out by using the GAUSSIAN09 suite of programs in gas-phase at the B3LYP/6-31G(d) levele,[5] respectively.

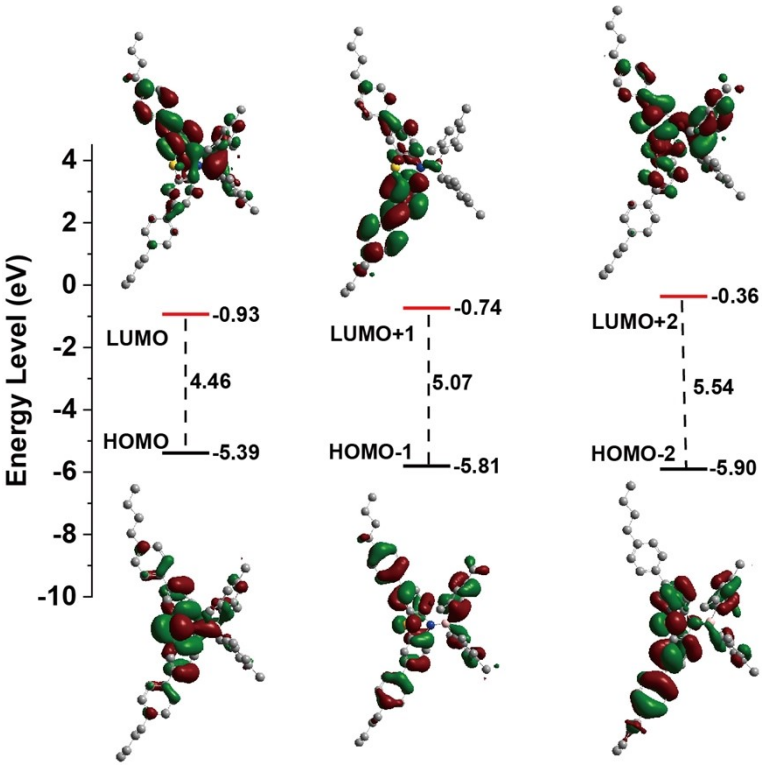

Figure S12. Computed molecular orbital plots for **4a**.

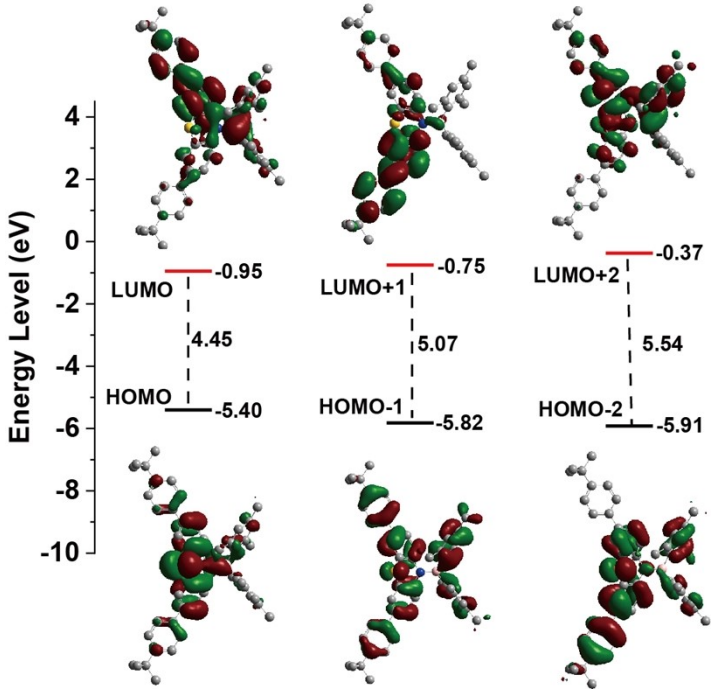

Figure S13. Computed molecular orbital plots for **4b**.

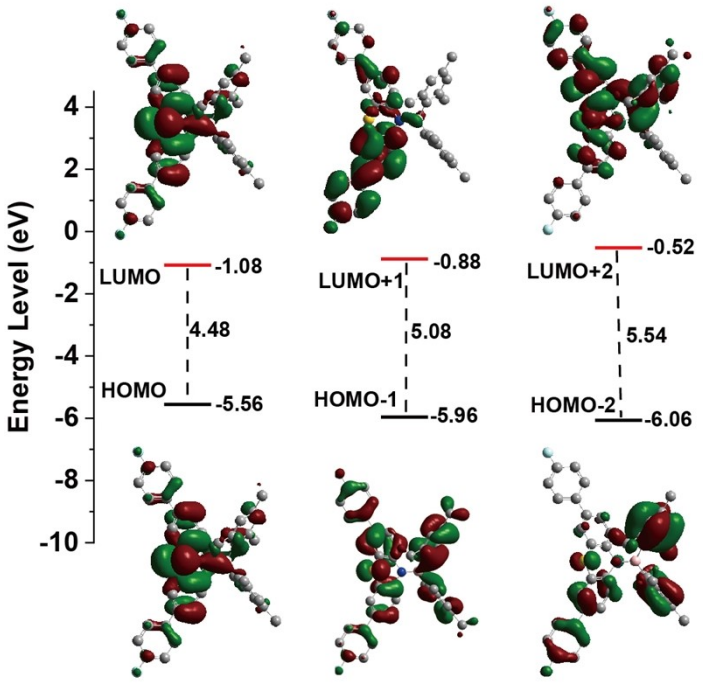

Figure S14 Computed molecular orbital plots for **4c**.

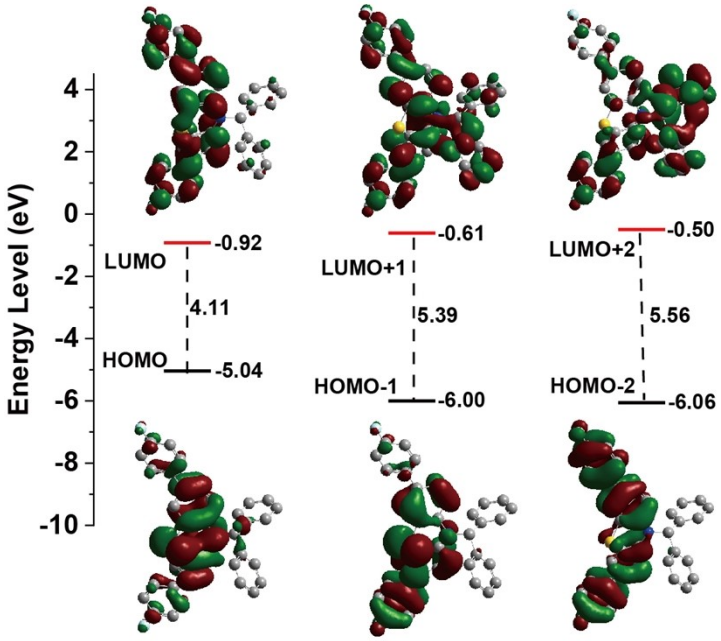

Figure S15 Computed molecular orbital plots for **4d**.

6. Determination of the detection limit

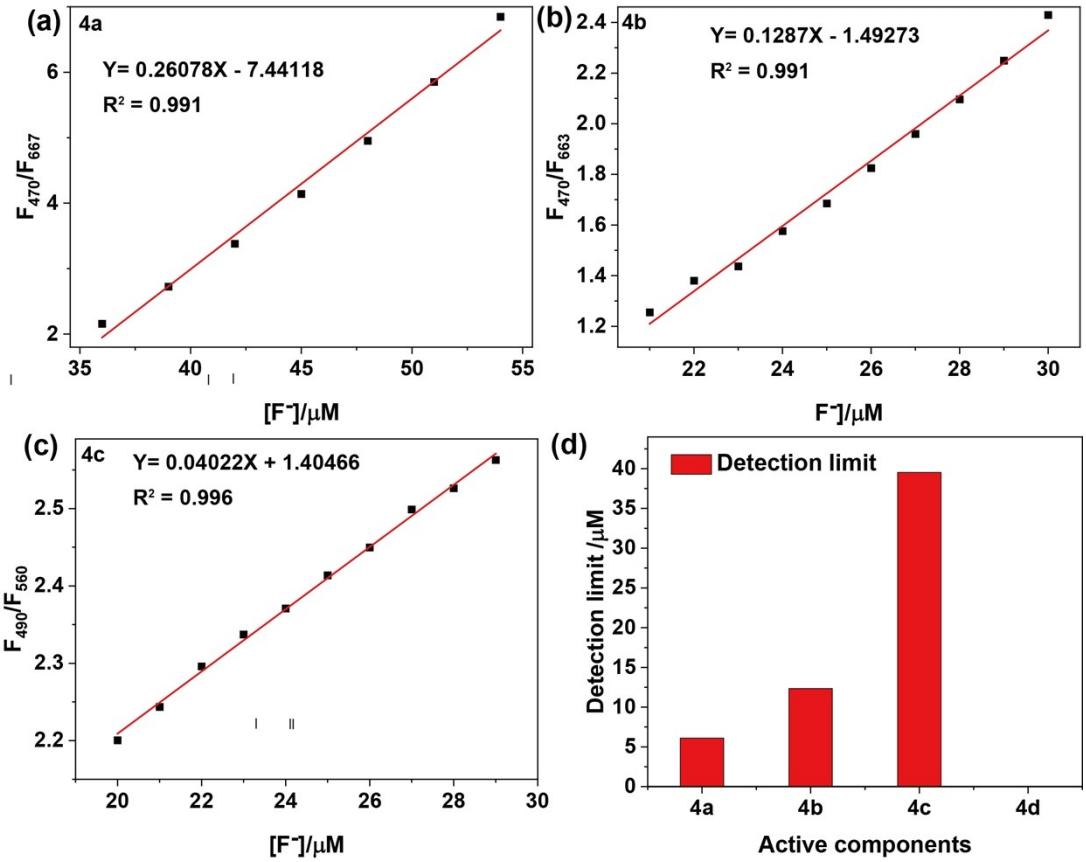

Figure S16 (a-c) The calibration curves and linear equation of **4a-4c** for FL intensity ratio changes upon gradual addition of F^-. (d)The calculated detection limits of **4a**, **4b**, and **4c**.

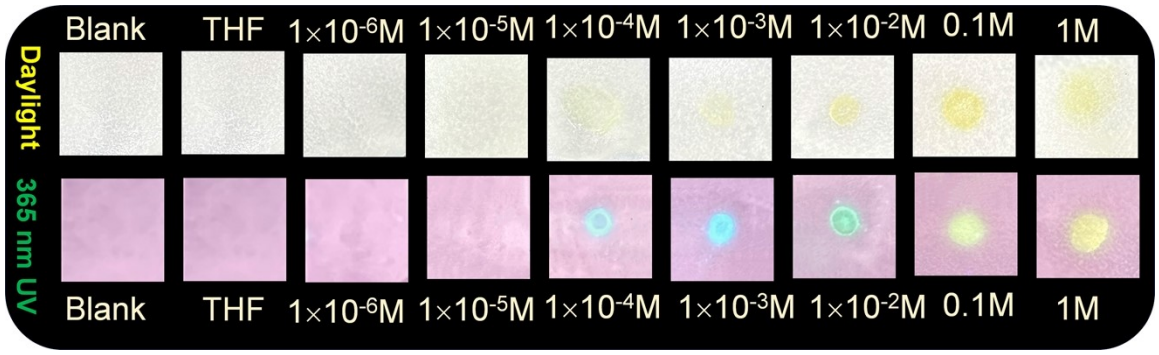

Figure S17. The **4a**-based film for F^- detection under daylight (up) and 365 nm UV irradiation (down).

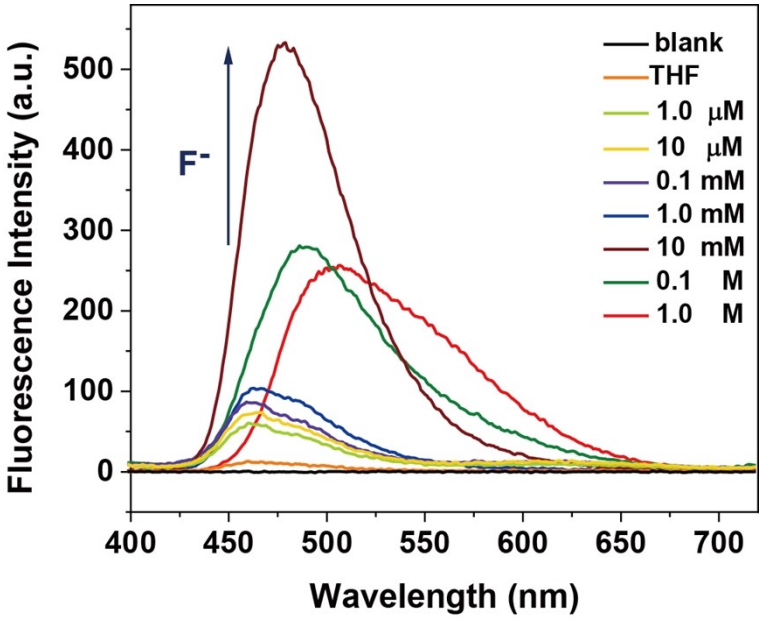

Figure S18. Spectral changes in the fluorescence of film based on **4a** after addition of TBAF.

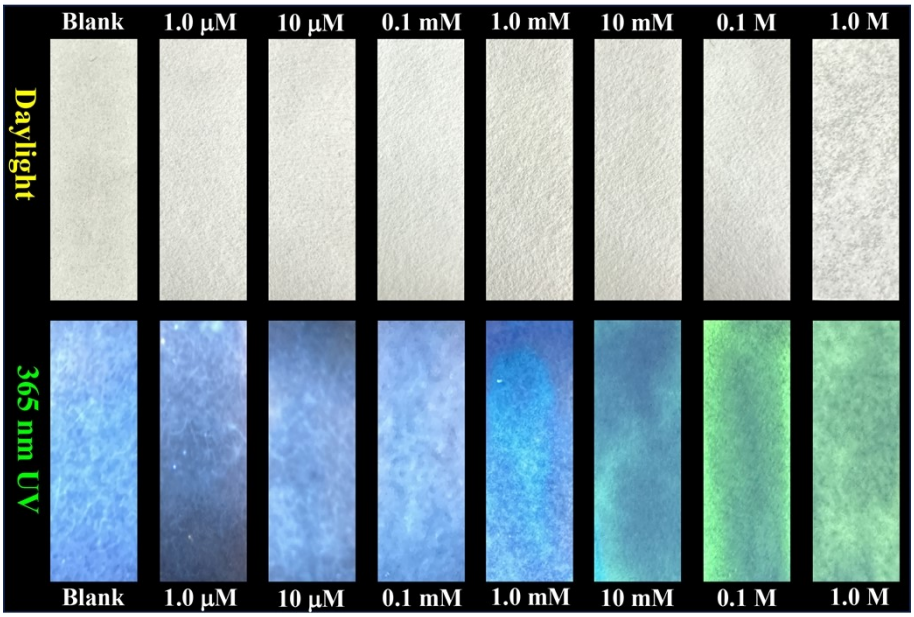

Figure 19. Photographs of **4a**-based test strips for F^- detection in aqueous solution under daylight (up) and 365 nm UV irradiation (down).

7. Complexation of 4b and 4c with different anions.

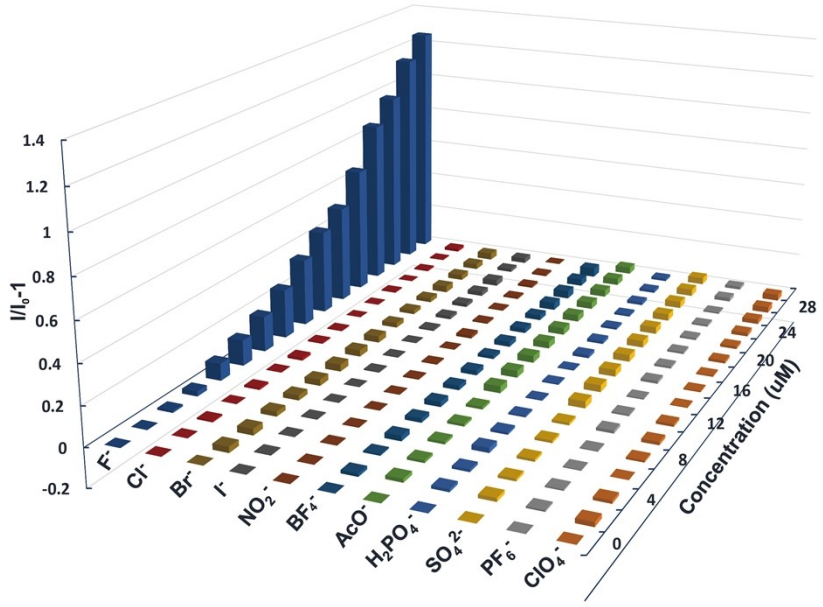

Figure S20. (I/I_0)-1 of F^- and other anions for the emission of **4b** in THF (10 μM) at different equivalents of anions.

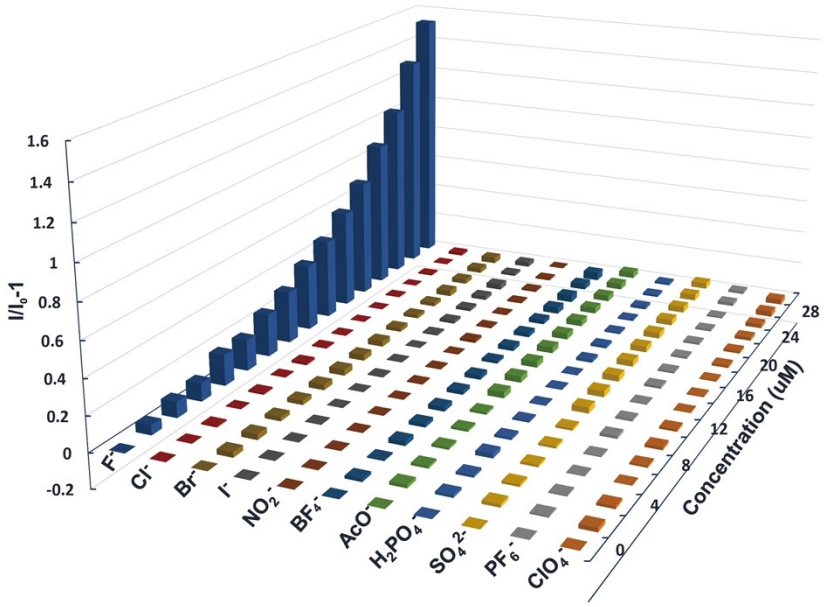

Figure S21. (I/I_0)-1 of F^- and other anions for the emission of **4c** in THF (10 μM) at different equivalents of anions.

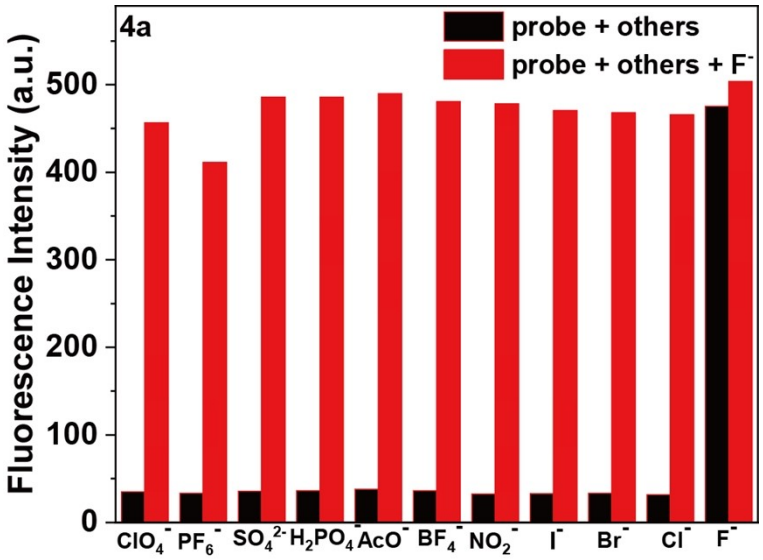

Figure S22. Interference experiments of **4a** (10 μM) in THF at 470 nm for F^- in the presence of other anions. The black bars represent the addition of the corresponding others ion, the red bars represent the change of the emission that occurs upon the subsequent addition of F^- to the above solution.

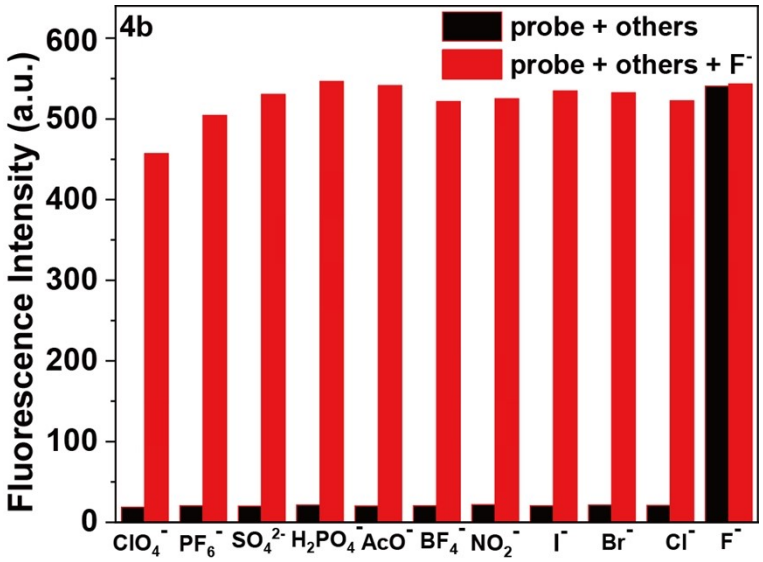

Figure S23. Interference experiments of **4b** (10 μM) in THF at 480 nm for F^- in the presence of other anions. The black bars represent the addition of the corresponding others ion, the red bars represent the change of the emission that occurs upon the subsequent addition of F^- to the above solution.

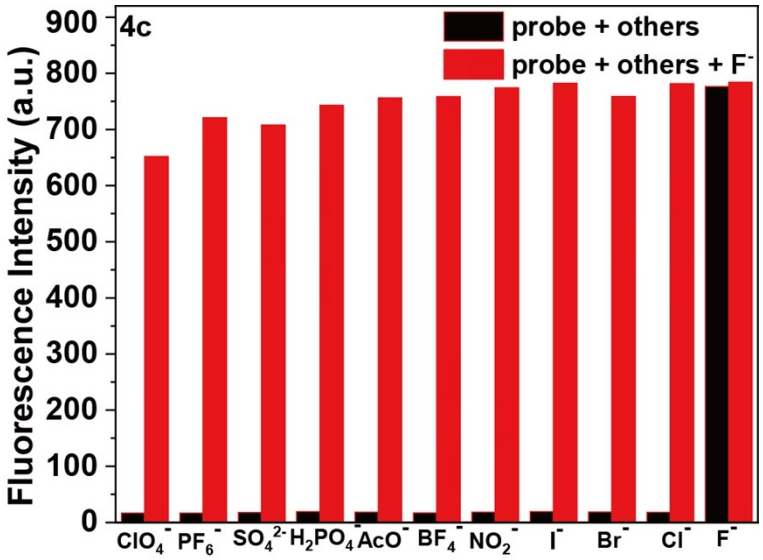

Figure S24. Interference experiments of **4c** (10 μM) in THF at 490 nm for F^- in the presence of other anions. The black bars represent the addition of the corresponding others ion, the red bars represent the change of the emission that occurs upon the subsequent addition of F^- to the above solution.

8. ^{1}H NMR and ^{13}C NMR spectra

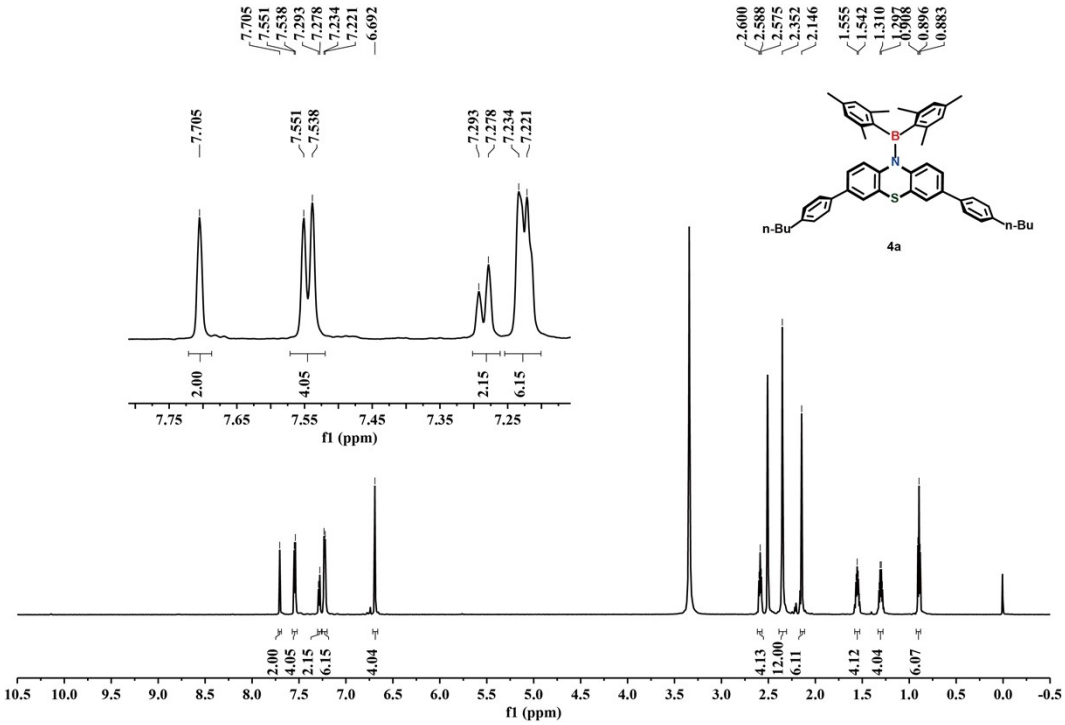

^{1}H NMR spectrum of **4a** in DMSO

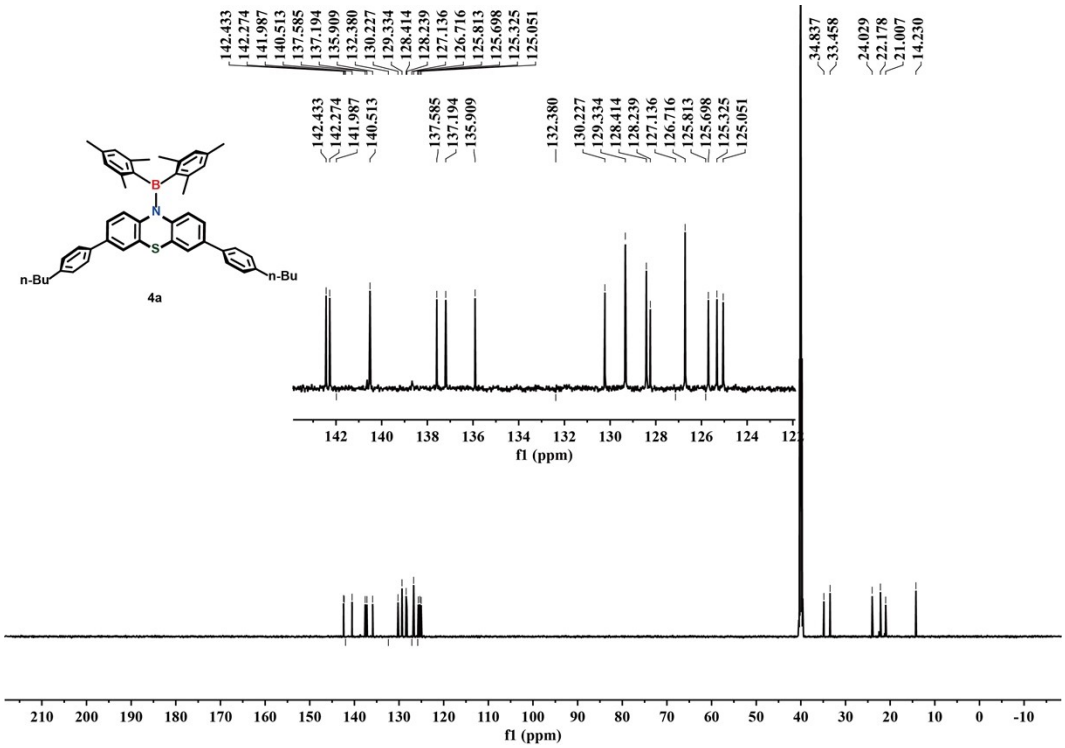

^{13}C NMR spectrum of **4a** in DMSO

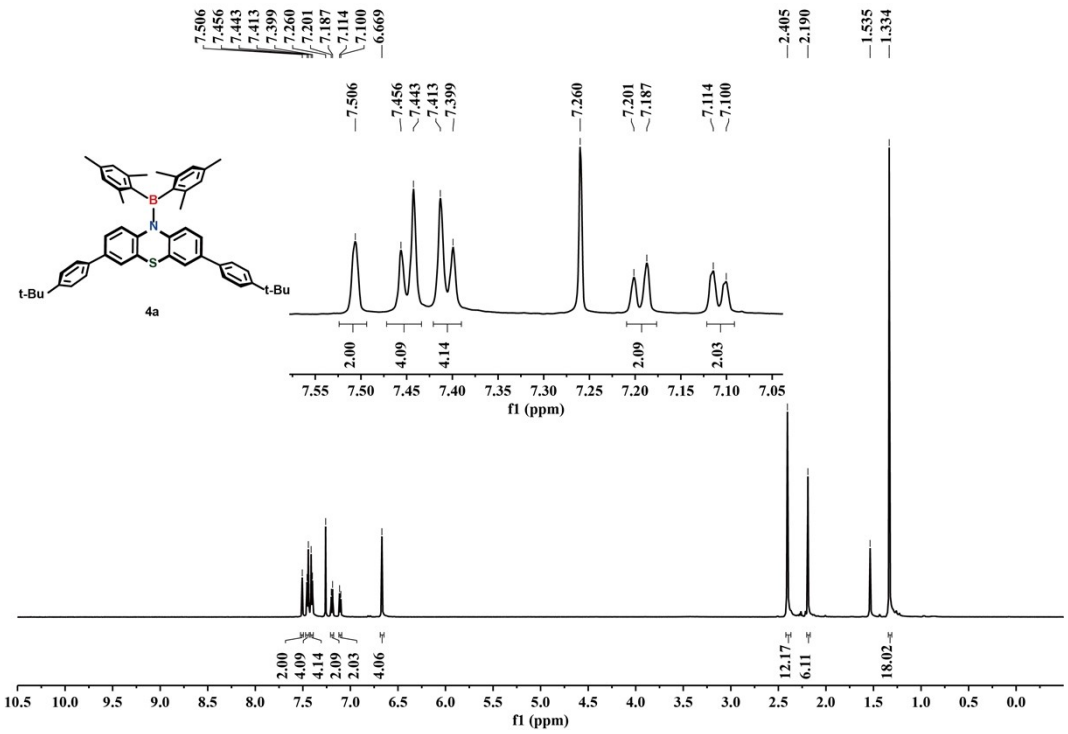

^{1}H NMR spectrum of **4b** in $CDCl_3$

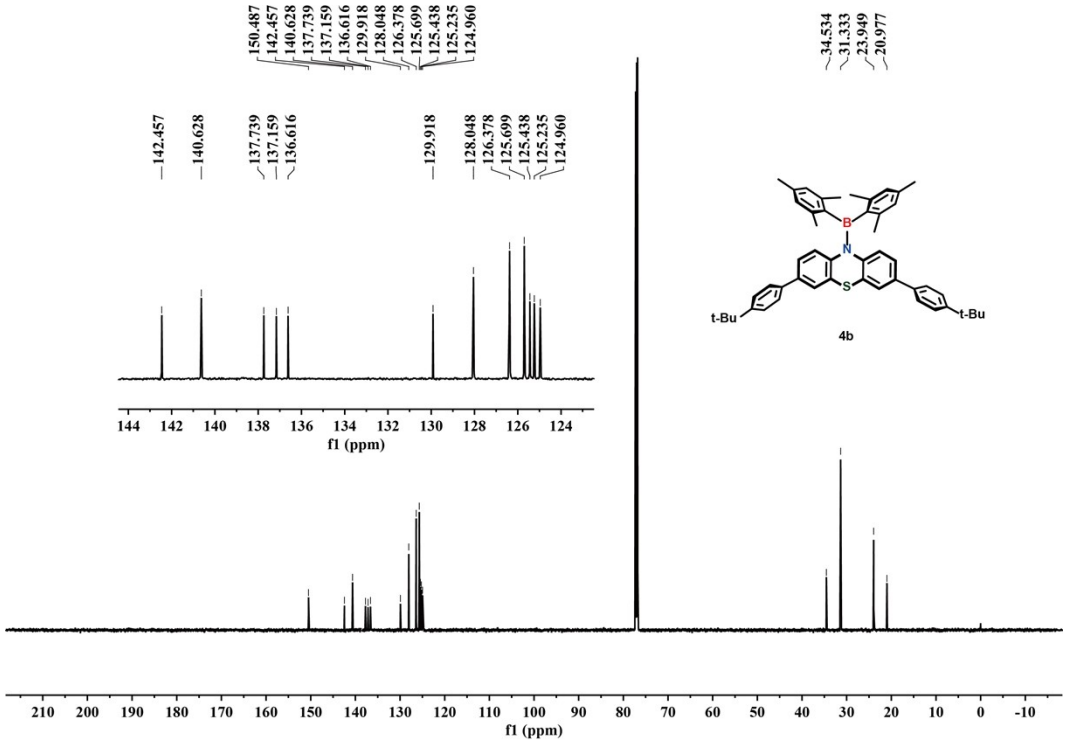

^{13}C NMR spectrum of **4b** in $CDCl_3$

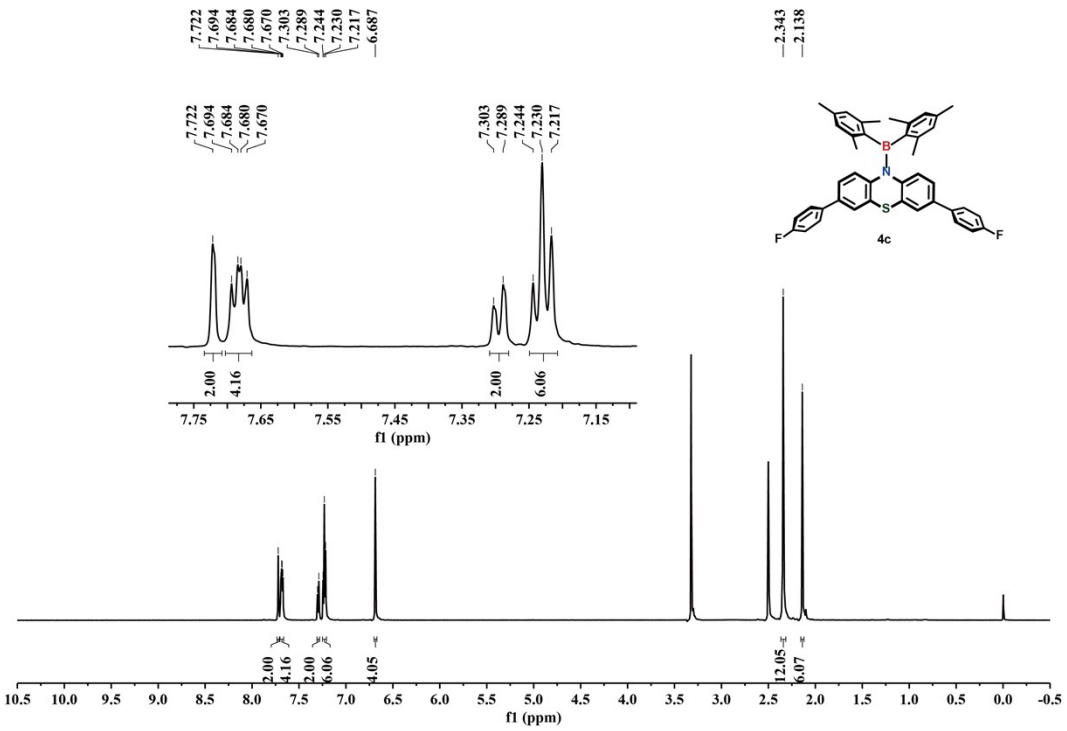

^{1}H NMR spectrum of **4c** in DMSO

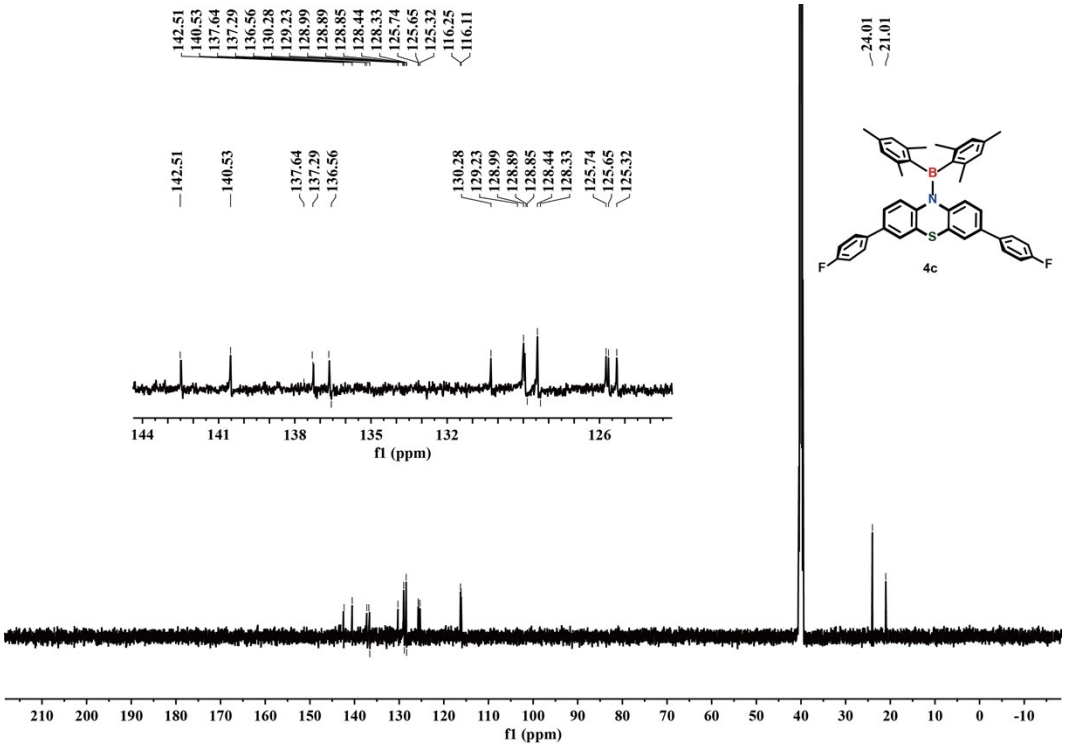

^{13}C NMR spectrum of **4c** in DMSO

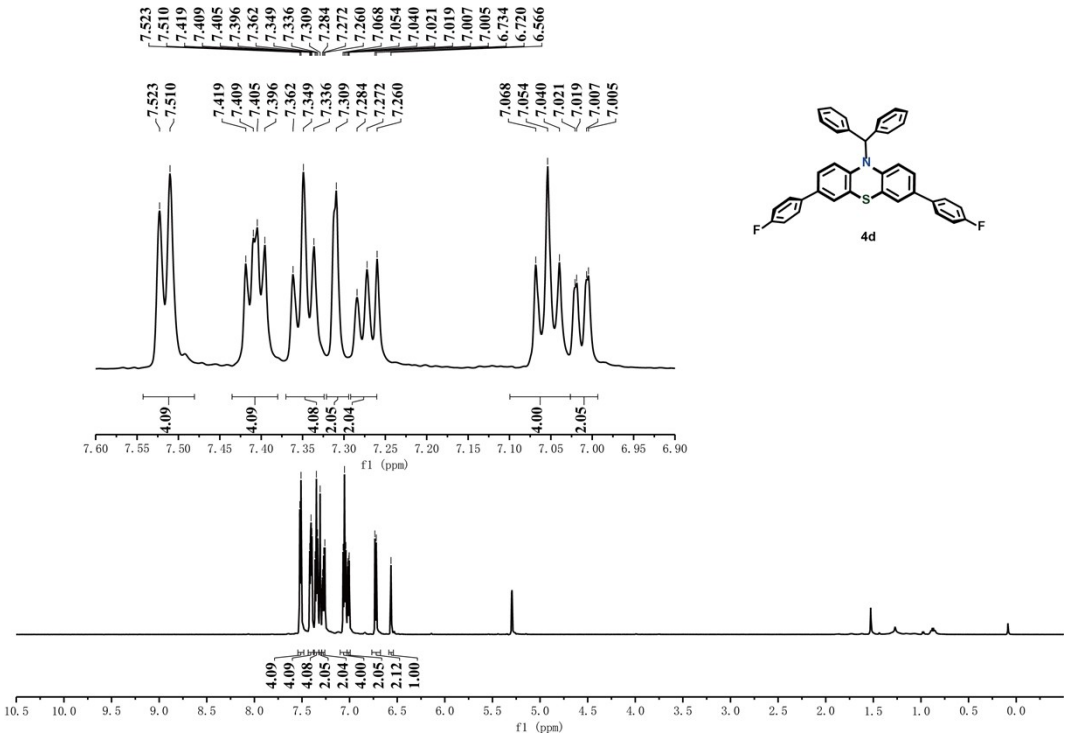

^{1}H NMR spectrum of **4d** in $CDCl_3$

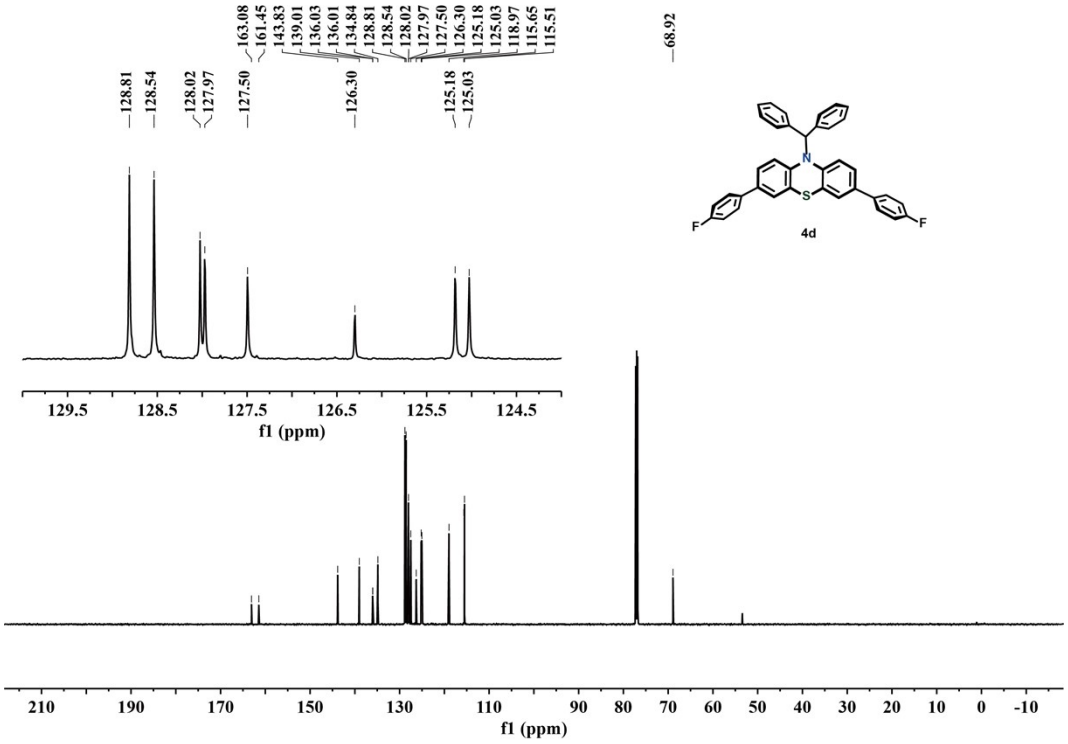

^{13}C NMR spectrum of **4d** in $CDCl_3$

9. HRMS spectra

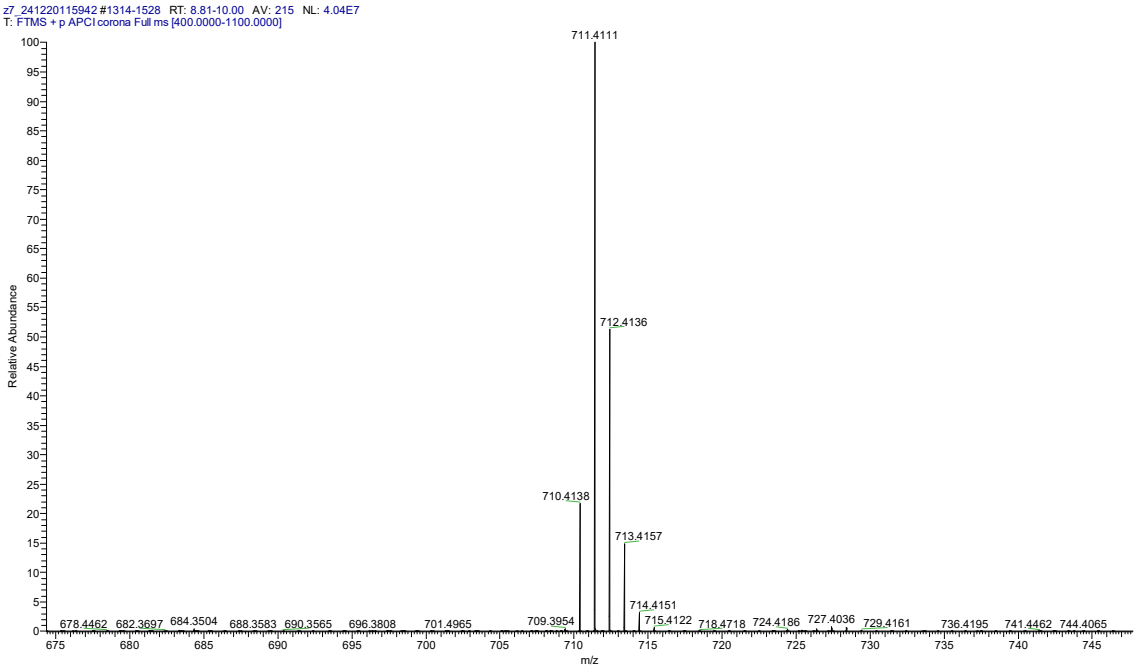

HRMS of **4a**

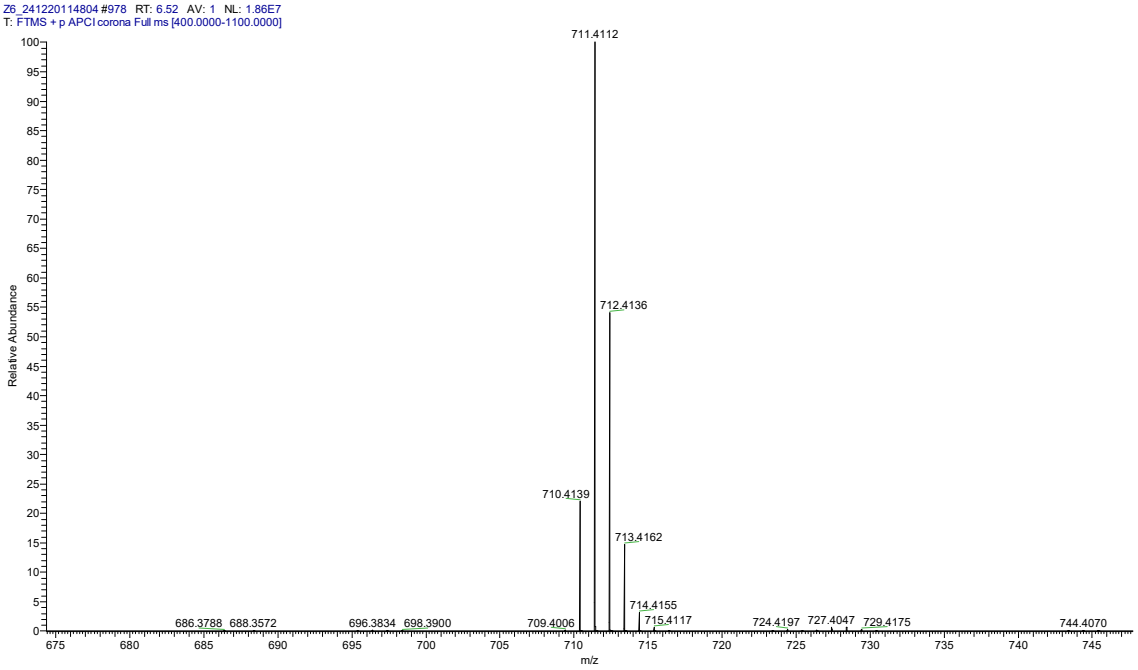

HRMS of **4b**

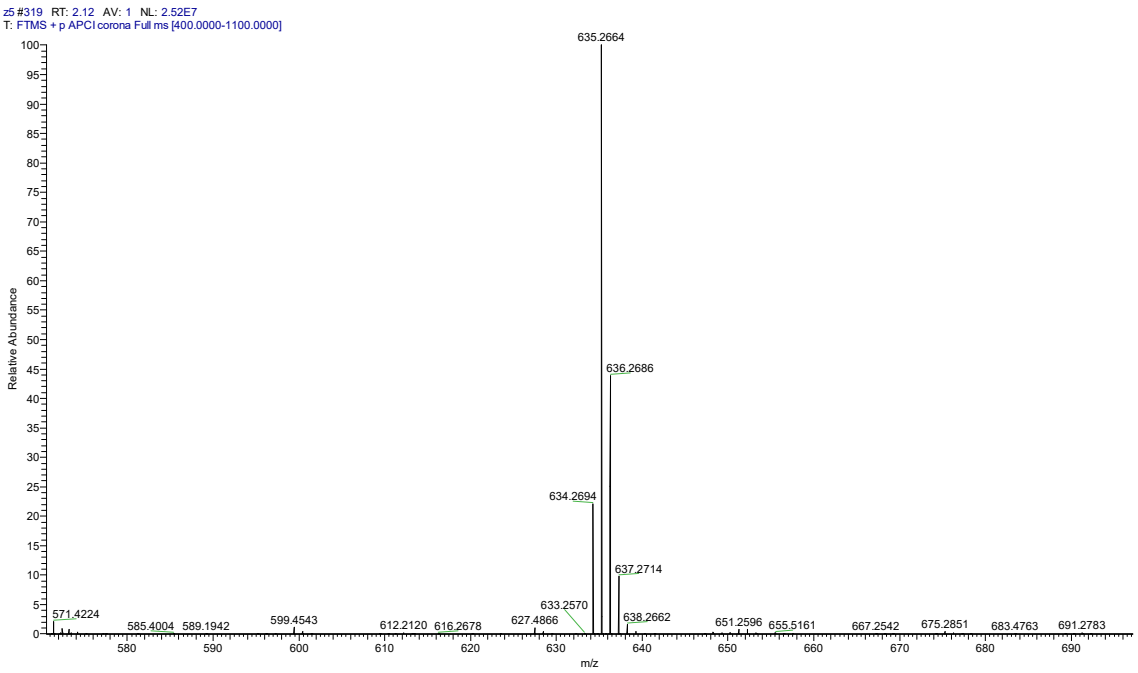

HRMS of **4c**

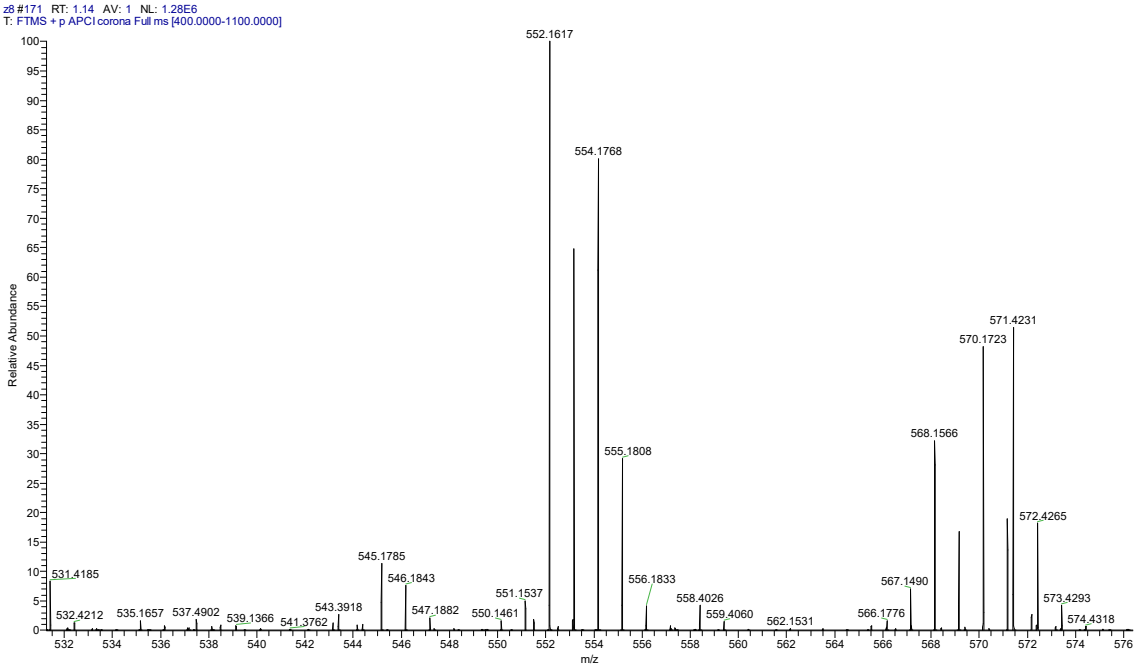

HRMS of **4d**

Author Contributions

Weidong Zhang conceived the idea for the study. Yan Wang and Guoqiang Li prepared the samples and conducted characterizations. Zengheng Wen, Zhuang Luo, Qiangqiang Jia helped to prepare and characterize the samples. Yan Wang, Guoqiang Li, and Weidong Zhang wrote the manuscript, and all the authors revised and polished the manuscript.

10. Reference

(1) Miertusˇ, S.; Scrocco, E.; Tomasi, J. *Chem. Phys.* **1981**, *55*, 117.

(2) Cammi, R.; Tomasi, J. J. *Comput. Chem.* **1995**, *16*, 1449.

(3) Tomasi, J.; Persico, M. *Chem. Rev*. **1994**, *94*, 2027.

(4) Cramer,C. J.; Truhlar, D. G. *Chem. Rev*. **1999**, *99*, 2161.

(5) Frisch, M. J.; Trucks, G. W.; Schlegel, H. B. Gaussian09, Revision A.01, Gaussian, Wallingford, Con, USA, **2009**.